

Radiation Physics and Engineering 2026; ?(?):?–?

COMSOL simulation study of electrostatic quadrupole doublet field characteristics in the ES-200 accelerator

Mohammad Mahdi Mansouri Hasanabadi^a, Hamidreza Mirzaei^{b,*}

^aRadiation Application Department, Shahid Beheshti University, G.C, Iran

^bDepartment of Physics and Accelerators, Nuclear Science and Technology Research Institute (NSTRI), P.O. Box 14395-836, Tehran, Iran

HIGHLIGHTS

-
-
-
-
-

ABSTRACT

This work presents a systematic optimization of an electrostatic quadrupole (ESQ) doublet designed for the ES200, a 200 keV Cockcroft-Walton ion accelerator through high-fidelity COMSOL Multiphysics simulations. The study aims to enhance beam focusing performance by rigorously analyzing critical field characteristics, including field linearity, electric potential distribution, and fringe field effects. Aperture diameters ranging from 30 mm to 70 mm were evaluated while maintaining a fixed electrode radius of 22 mm, consistent with mechanical and electrical constraints. The optimized configuration, featuring a 50 mm aperture, demonstrated superior field linearity with a minimal relative deviation of 0.8% at a 10 mm radial distance, ensuring uniform focusing forces across the beam profile. Furthermore, the implementation of integrated shielding discs and a structural support frame resulted in a 37.5% reduction in fringe field leakage, thereby improving field confinement and overall beam stability. These findings provide a validated design framework for fabricating a high-performance ESQ doublet, contributing to enhanced beam quality and operational reliability in compact, low-energy ion accelerator systems.

KEYWORDS

Electrostatic quadrupole
ESQ doublet
Ion accelerator
Beam focusing
COMSOL simulation
ES200

HISTORY

Received:
Revised:
Accepted:
Published:

1 Introduction

The Oxford electrostatic microprobe, used for proton therapy, delivers a scant $0.05 \mu\text{A}\cdot\text{cm}^{-2}$ due to excessive beam divergence (Watt et al., 1982). This low current density can't target tumors smaller than a millimeter, missing cancer-killing precision (Watt et al., 1982). With an ESQ lens, that leaps to $10 \mu\text{A}\cdot\text{cm}^{-2}$, locking in deadly accuracy. Such focusing demands closer scrutiny. Electrostatic quadrupole (ESQ) lenses steer charged particles via electric fields, offering versatile focusing in singlets, doublets, or triplets (Enge, 1967). Modern designs optimize beam precision for therapy, implantation, and spectroscopy (Hinterberger, 2008; Mirzaei et al., 2025), outpacing magnetic systems in compactness. Electrostatic accelerators

kicked off with Cockcroft-Walton's 1930s nuclear feats (Cockcroft and Walton, 1930), followed by Van de Graaff's high-voltage innovations (Van de Graaff, 1931). ESQs emerged in the 1960s for sharper beam control (Guharay et al., 2003; Ziegler, 1986), with early adopters tackling ion implantation and scattering (Humphries, 2013). By the 1980s, ESQs honed microprobe precision (Watt et al., 1982; Legge et al., 1979), while 21st-century advances refined BNCT and fusion beams (Taskaev et al., 2021; Kwan et al., 1994). Recent compact setups, including laser-driven systems, push therapy frontiers (Scisciò et al., 2018; Bieniosek et al., 2005), building on decades of optics progress. The ESQ doublets performance in compact accelerators like the ES200 depends on multiple field characteristics, including field linearity, potential profiles, and

*Corresponding author: mirzaee.mine@gmail.com

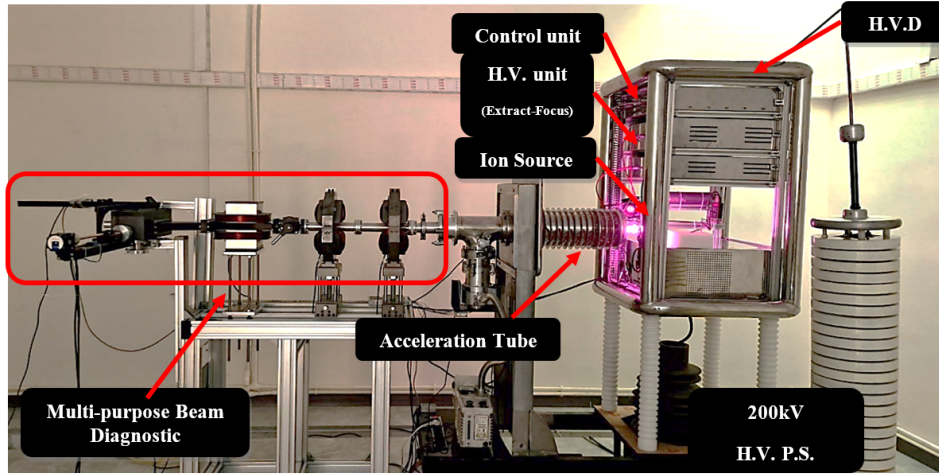


Figure 1: The 200 keV Cockcroft-Walton accelerator installed in laboratory of the physics and accelerator research school.

fringe field effects. Field linearity ensures uniform focusing forces, while controlled fringe fields and potential distributions enhance beam stability and structural design-key factors for improving quadrupole performance. This study evaluates these properties to optimize the ESQ doublet's design, paving the way for its fabrication and integration into the ES200 to achieve enhanced focusing and stability.

2 The ES200 Accelerator

The ES200 (Fig. 1), a 200 keV electrostatic Cockcroft-Walton ion accelerator has been successfully designed, constructed, and tested at the Nuclear Science and Technology Research Institute (NSTRI) in Iran. The system comprises a 13.56 MHz RF ion source, a high-voltage acceleration column, and a versatile beam transport and diagnostic setup. Key achievements include a maximum beam current of $600 \mu\text{A}$ in continuous operation, focused beam profiles with RMS sizes of 4.2 mm (x) and 3.8 mm (y) at 150 keV, and reliable operation in both continuous and pulsed modes with pulsed beam currents up to 1.5 mA. The multi-purpose diagnostic system, equipped with quadrupole and dipole magnets, enables precise measurement of beam current, divergence, emittance, and momentum spectrum. This accelerator demonstrates stable and safe performance in generating, accelerating, and diagnosing low-energy ion beams, showing high potential for research and industrial applications such as ion implantation, materials science, and nuclear studies (Mirzaei et al., 2025). Key specifications, drawn from the accelerator's performance analysis, are summarized in Table 1 (Mirzaei et al., 2025).

Table 1: The specification of the 200 keV electrostatic accelerator.

Ion Species	Gases ions (proton, He, O, N, etc.)
Acceleration Voltage	<200 kV
Beam Current Max.	<1 mA
Energy Stability	<0.5%
Operation Time without Maintenance	>2000 h

3 Methods and Materials

The ESQ doublet consists of four cylindrical electrodes positioned symmetrically to generate a quadrupole field for beam focusing in compact accelerators. In an ideal quadrupole, the electric field is given by $E_x = \frac{2V}{G_0^2}x$ and $E_y = -\frac{2V}{G_0^2}y$, where V is the applied voltage and G_0 is the aperture diameter, with the ratio of electrode radius to aperture diameter r_e/G_0 determining field linearity (optimal at 1.147) (Edwards and Syphers, 2008). The model was designed with $r_e = 22$ mm and G_0 varying from 30 to 70 mm, considering fabrication constraints such as electrode spacing to prevent electrical breakdown. For the minimum gap ($G_0 = 30$ mm), the simulated peak electric field at 10 kV is $2.36 \text{ MV}\cdot\text{m}^{-1}$, which remains below the air breakdown threshold ($\sim 3 \text{ MV}\cdot\text{m}^{-1}$), providing a conservative safety margin. This field level is also compatible with the focusing requirements in the intended accelerator energy range. The applied voltage is selected based on beam energy and desired final beam size, with 8 kV determined through parametric studies for our ~ 150 keV beam. The 22 mm electrode radius balances field linearity, manufacturability, and breakdown voltage, and was used to optimize the aperture diameter.

Figure 2 illustrates the ESQ doublet geometry, showing the electrode and aperture configuration. Simulations were performed using COMSOL Multiphysics at 8 kV with a mesh size of 0.1 mm, chosen to balance computational accuracy and efficiency (negligible field variation with finer meshes). The electric field E_{sim} along the x -direction was extracted for each aperture to assess field linearity, potential profiles, and fringe field effects, focusing on a typical beam radius of around 10 mm as a reference for the ES200. Field linearity was evaluated by fitting a linear trend $E_{fit} = g_E \cdot x$ to E_{sim} , where g_E is the field gradient derived from the fit, within a defined linear range. This linear range was determined through a range analysis, where we iteratively tested different radial ranges to identify the largest one where the relative absolute deviation $|E_{sim} - E_{fit}|/E_{fit}$ remains below 5%. This 5%

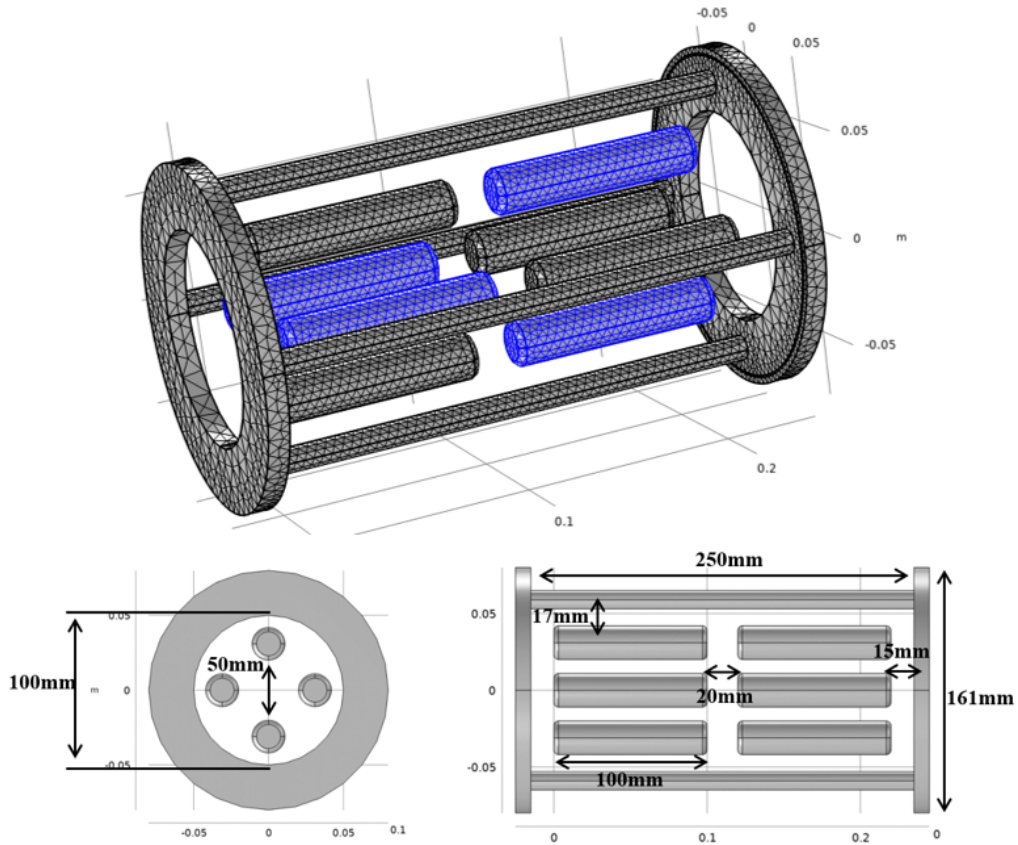


Figure 2: ESQ doublet geometry, illustrating the electrode and aperture configuration.

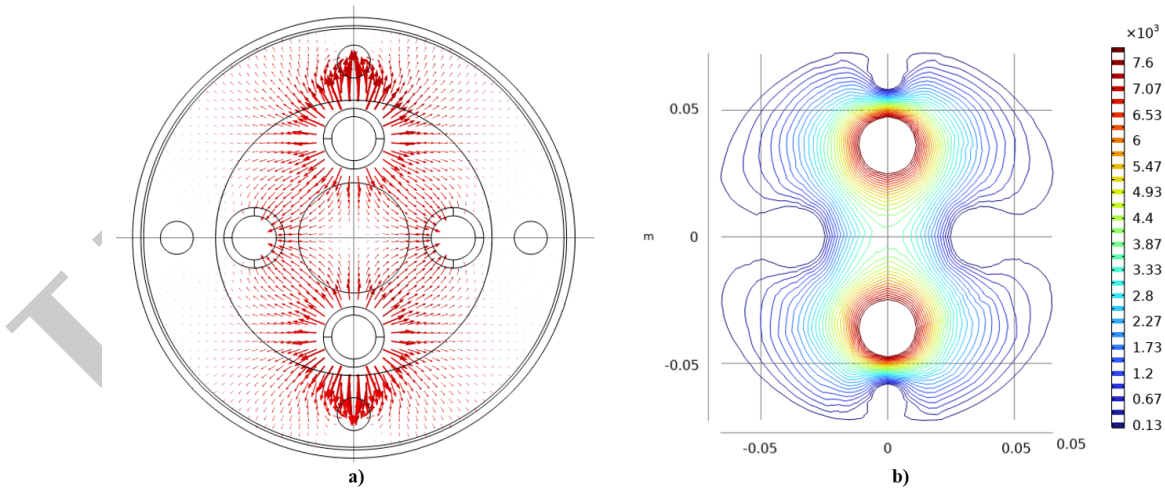


Figure 3: Potential profiles: (a) field vectors and (b) equipotential contours in x-y plane at 14 kV.

threshold balanced practical focusing needs with simulation accuracy, as higher thresholds (e.g., 10%) permitted excessive non-linearities, while lower ones (e.g., 2%) overly restricted the linear range. The fit was applied only within this linear range (e.g., 1 to 10 mm for 30 mm, up to 1 to 25 mm for 70 mm) to avoid errors in g_E from non-linear regions. Deviations were calculated across the entire range to evaluate field behavior, while axial potential profiles were analyzed to quantify fringe field effects. The simulated model shown in Fig. 2.

4 Simulation Results

This section presents the ESQ doublet’s electric field properties through COMSOL simulations at 8 kV with 22 mm electrodes.

4.1 Potential Profiles and Field Distribution

Figure 3 shows the field profile: (a) field vectors and (b) equipotential contours in the $x - y$ midplane, confirming quadrupole functionality for beam shaping in the ES200.

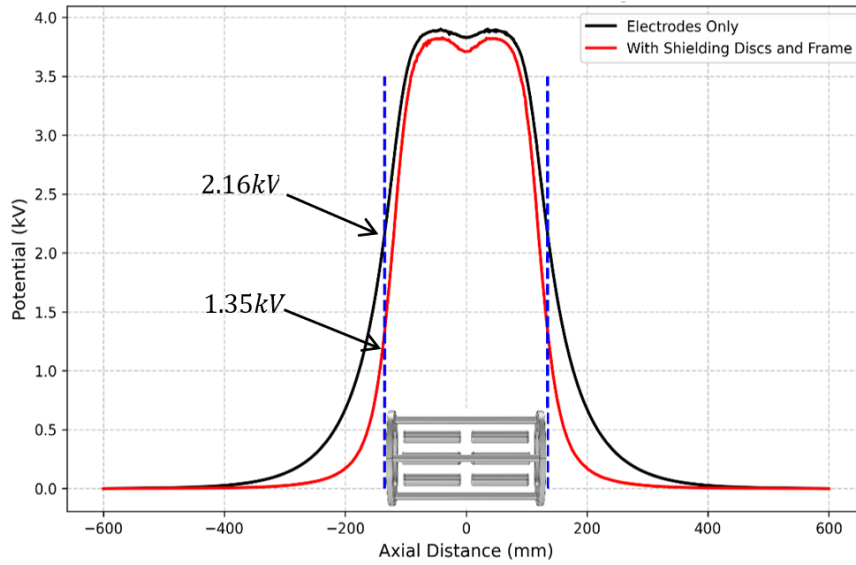


Figure 4: Axial potential profiles with (red) and without (black) discs and frame, showing a reduction in fringe field leakage.

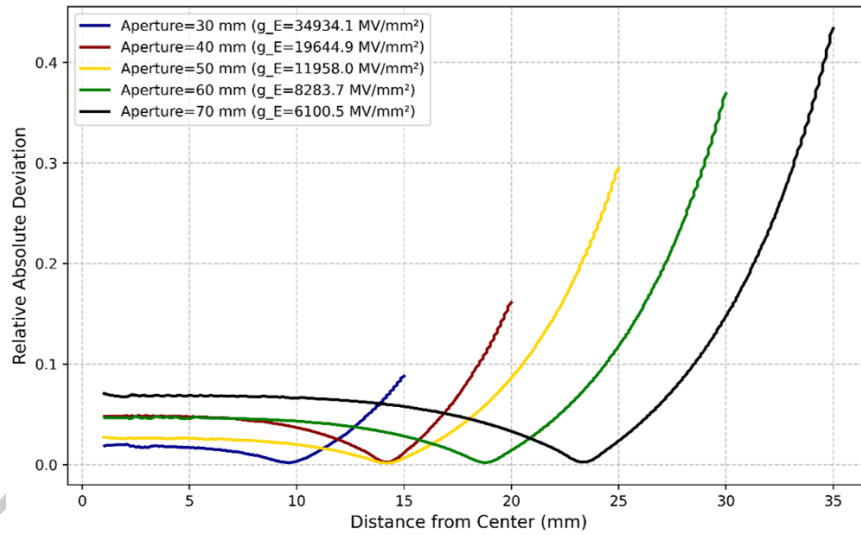


Figure 5: Relative absolute deviation from fitted linearity (normalized by E_{fit}) for apertures 30, 40, 50, 60, 70 mm.

Considering the electric field vector directions in the figure below, the quadrupole function is easily observable. The vector direction is towards the center in the vertical direction and outwards from the center in the horizontal direction, with their magnitudes decreasing as they approach the center of the circle. This is also evident in the equipotential lines, which increase in magnitude closer to the electrodes.

Table 2: Linear range, field gradient, and deviation for aperture sizes (G_0).

G_0 (mm)	Linear Range (mm)	g_E ($MV \cdot mm^{-2}$) $\times 10^3$	Deviation at 10 (mm)
30	1 to 10	34.9	0.9%
40	1 to 15	19.6	1.5%
50	1 to 15	12.0	0.8%
60	1 to 20	8.3	1.5%
70	1 to 25	6.1	1.6%

4.2 Fringe Field Effects

Figure 4 compares axial potential profiles with and without shielding discs and frame, showing the potential variation along the z-axis near the ESQ edges (from $z = -600$ mm to 600 mm) and a reduction in fringe field leakage in the regions outside the quadrupole structure. The axial potential at the quadrupole entrance, despite the presence of the shielding disk, has been reduced from 2.16 kV to 1.35 kV.

4.3 Field Linearity with Aperture Size

Figure 5 plots the relative absolute deviation $|E_{sim} - E_{fit}|/E_{fit}$ for apertures 30 to 70 mm, showing how the field deviates from linearity with radial distance, with g_E fitted in each linear range as defined in the range analysis. Table 2 lists the linear ranges, fitted field gradients g_E , and deviations at 10 mm for each aperture, derived

from the simulation data. Figure 6 compares deviations at 10 mm across all apertures (0.8%-1.6%), highlighting the linearity trend. The electrode radius $r_e = 22$ mm was selected based on a similar linearity trend for 18-24 mm.

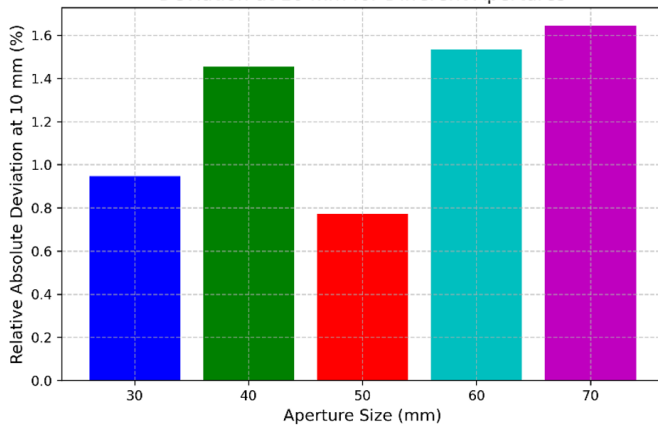


Figure 6: Deviation at 10 mm for apertures 30, 40, 50, 60, 70 mm.

5 Discussion

The simulation results provide insights into the ESQ doublet's field properties for the ES200 accelerator. Figure 4 shows a 37.5% reduction in fringe field leakage with shielding discs and frame, enhancing field control and beam stability—a practical feature for quadrupole design, which can be further explored in future studies to assess its impact on beam dynamics. Figure 5 illustrates the relative absolute deviation ($|E_{sim} - E_{fit}|/E_{fit}$) for apertures 30 to 70 mm, with g_E fitted in each linear range as described earlier. Deviations are low within linear regions (0.8%-1.6% at 10 mm, Table 2) but rise sharply beyond these ranges. The 40 mm aperture exhibits a higher deviation (1.5% at 10 mm) than the 50 mm aperture (0.8%), despite its geometry being closer to the optimal configuration for linearity. This suggests slight non-linearities in the 40 mm aperture's field within its linear range (1 to 15 mm), possibly due to a steeper potential gradient from its smaller size, while the 50 mm aperture's larger diameter may yield a more linear field. The 30 mm aperture, with a geometry even closer to optimal, shows a lower deviation (0.9%), as expected. The 40 mm and 60 mm apertures both have a deviation of 1.5% at 10 mm, indicating similar non-linear effects despite their differing configurations. Beyond the linear range, the 40 mm aperture's deviation is lower than the 50 mm, consistent with its more favorable geometry and higher g_E (19.6 MV.mm⁻² vs. 12.0 MV.mm⁻²), reducing relative deviation. While these observations provide a preliminary understanding, a theoretical model of field distribution may offer a definitive explanation for the 40 mm aperture's behavior in future studies. As explained in the methods section, the 5% deviation threshold for defining linear ranges balanced practical focusing needs with simulation accuracy, while fitting only within these ranges avoided errors from non-linear regions. These findings guide the optimized design, incorporating a shielding

disc that reduces fringe field leakage by 37.5% while also serving as a structural holder and centering mechanism when connected to a frame. The 50 mm aperture, with a low deviation of 0.8% at 10 mm and good linear behavior in the operational range, was selected to ensure effective field linearity and stability for the ES200. This approach establishes a solid foundation for achieving reliable quadrupole performance in compact accelerator systems.

6 Conclusions

This study successfully evaluated the electric field properties of an ESQ doublet to optimize its design for the ES200 accelerator. By analyzing field linearity, potential profiles, and fringe field effects through COMSOL simulations, the research identified a configuration that balances effective beam focusing with practical fabrication constraints, incorporating structural components to enhance field control and alignment. The findings provide a robust foundation for improving quadrupole performance in compact accelerators, offering a pathway for enhanced beam stability and precision in future implementations.

Conflict of Interest

The authors declare no potential conflict of interest regarding the publication of this work.

Funding

The authors declare that no funds, grants, or other financial support were received during the preparation of this manuscript.

References

- Bieniosek, F., Celata, C., Henestroza, E., et al. (2005). 2-MV electrostatic quadrupole injector for heavy-ion fusion. *Physical Review Special Topics Accelerators and Beams*, 8(1):010101.
- Cockcroft, J. D. and Walton, E. T. (1930). Experiments with high velocity positive ions. *Proceedings of the royal society of London. Series A, containing papers of a mathematical and physical character*, 129(811):477–489.
- Edwards, D. A. and Syphers, M. J. (2008). *An introduction to the physics of high energy accelerators*. John Wiley & Sons.
- Enge, H. A. (1967). Focusing of charged particles. *Deflecting Magnets*, 2:203–264.
- Guharay, S., Nishiura, M., Sasao, M., et al. (2003). Focusing of He⁺ beams using a compact electrostatic quadrupole lens system. *Nuclear Instruments and Methods in Physics Research Section A: Accelerators, Spectrometers, Detectors and Associated Equipment*, 496(2-3):239–247.
- Hinterberger, F. (2008). *Physics of particle accelerators and ion optics*. 2.

Humphries, S. (2013). *Charged particle beams*. Courier Corporation.

Kwan, J. W., Anderson, O. A., Reginato, L. L., et al. (1994). Electrostatic quadrupole DC accelerators for BNCT applications.

Legge, G., McKenzie, C., and Mazzolini, A. (1979). The Melbourne proton microprobe. *Journal of Microscopy*, 117(2):185–200.

Mirzaei, H., Sanaye, S., Yadollahzadeh, B., et al. (2025). Development and performance analysis of the 200 keV Cockcroft-Walton ion accelerator. *Results in Physics*, 68:108089.

Scisciò, M., Migliorati, M., Palumbo, L., et al. (2018). Design and optimization of a compact laser-driven proton beamline. *Scientific Reports*, 8(1):6299.

Taskaev, S., Berendeev, E., Bikchurina, M., et al. (2021). Neutron source based on vacuum insulated tandem accelerator and lithium target. *Biology*, 10(5):350.

Van de Graaff, R. J. (1931). A 1,500,000 volt electrostatic generator. *Phys. Rev.*, 38:1919.

Watt, F., Grime, G., Blower, G., et al. (1982). The Oxford 1 μm proton microprobe. *Nuclear Instruments and Methods in Physics Research*, 197(1):65–77.

Ziegler, J. F. (1986). Stopping and range of ions in solids. In *Inelastic near-surface interactions. Proceedings of the Werner Brandt workshop*, number CONF-8404190–, pages 284–284.

©2026 by the journal.

RPE is licensed under a [Creative Commons Attribution-NonCommercial 4.0 International License](#) (CC BY-NC 4.0).



To cite this article:

M. M. Mansouri Hasanabadi, H. Mirzaei. COMSOL simulation study of electrostatic quadrupole doublet field characteristics in the ES-200 accelerator. *Radiation Physics and Engineering*, In Press.

DOI:

To link to this article: